JACS
JOURNAL OF THE AMERICAN CHEMICAL SOCIETY
Article
pubs.acs.org/JACS

Single Molecule Force Spectroscopy Reveals That Iron Is Released from the Active Site of Rubredoxin by a Stochastic Mechanism

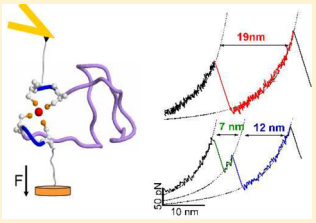
Peng Zheng,[†] Shin-ichi J. Takayama,[‡] A. Grant Mauk,[‡] and Hongbin Li*[,†]

[†]Department of Chemistry, University of British Columbia, Vancouver, British Columbia V6T 1Z1, Canada

[‡]Department of Biochemistry and Molecular Biology and the Center for Blood Research, University of British Columbia, Vancouver, British Columbia V6T 1Z3, Canada

Supporting Information

ABSTRACT: Metal centers in metalloproteins involve multiple metal−ligand bonds. The release of metal ions from metalloproteins can have significant biological consequences, so understanding of the mechanisms by which metal ion dissociates has broad implications. By definition, the release of metal ions from metalloproteins involves the disruption of multiple metal−ligand bonds, and this process is often accompanied by unfolding of the protein. Detailed pathways for metal ion release from metalloproteins have been difficult to elucidate by classical ensemble techniques. Here, we combine single molecule force spectroscopy and protein engineering techniques to investigate the mechanical dissociation mechanism of iron from the active site of the simplest iron−sulfur protein, rubredoxin, at the single molecule level. Our results reveal that the mechanical rupture of this simplest iron center is stochastic and follows multiple, complex pathways that include concurrent rupture of multiple ferric-thiolate bonds as well as sequential rupture of ferric-thiolate bonds that lead to the formation of intermediate species. Our results uncover the surprising complexity of the rupture process of the seemingly simple iron center in rubredoxin and provide the first unambiguous experimental evidence concerning the detailed mechanism of mechanical disruption of a metal center in its native protein environment in aqueous solution. This study opens up a new avenue to investigating the rupture mechanism of metal centers in metalloproteins with unprecedented resolution by using single molecule force spectroscopy techniques.



INTRODUCTION

The mechanical activation of chemical bonds is increasingly recognized as an important means by which chemical reactions can be activated and as a complement to the classical thermochemical, electrochemical, and photochemical activation processes.[1−4] The mechanical approach has provided new perspectives on the activation of chemical bonds and may reveal mechanistic information that is otherwise difficult to obtain by other methods.[1−7] The development of single molecule force spectroscopy techniques has enabled investigation of the mechanical activation of chemical bonds at the single molecule level, and pioneering studies have provided new insights into some important chemical reactions.[1,8−11]

Metalloproteins are ubiquitous in nature and play essential roles in a wide range of biological processes. Through the formation of multiple metal−ligand coordination bonds, metal centers are incorporated into metalloproteins to serve as structural and active sites that greatly expand the stability and functionality of proteins.[12,13] The mechanical rupture of metal−ligand bonds can lead to the disruption of these bonds and the release of metal ions from metalloproteins, which may ultimately lead to the unfolding of metalloproteins and result in significant biological consequences.[12,14−17] Understanding the mechanisms by which metal−ligand bonds in metalloproteins are disrupted and metal ions are released is not only of critical importance for the understanding of the functional properties of such proteins but may also offer new insights into the mechanisms by which metalloproteins fold.[15,18,19]

Spectroscopic signatures of metal−ligand bonds allow dissociation of metal−ligand bonds to be monitored at the ensemble level.[12,20−22] However, such classic methods cannot directly reveal either the dissociation of an individual metal−ligand bond or the sequence of events leading to the dissociation of multiple metal−ligand bonds. At present, the mechanistic complexity of the disruption of a metal center remains largely uncharacterized. Dissociation of many metal centers in metalloproteins has been shown to exhibit first-order kinetics, suggesting that the multiple metal−ligand bonds at these metal centers dissociate concurrently in an all-or-none fashion.[21,23−25]

Here, we use single molecule force spectroscopy techniques to investigate the mechanical rupture process of the $Fe(SCys)_4$ center in rubredoxin. Our results reveal that mechanical release of iron from the active site of this protein is complex and involves several pathways, both concurrent and sequential rupture of multiple ferric-thiolate bonds, that occur in parallel. This discovery that disruption of even the simplest of metal ion binding sites occurs by a stochastic mechanism provides new insight into the functional properties of such sites and the forces that stabilize them.

Received: February 28, 2013
Published: April 29, 2013

Downloaded via NANJING UNIV on July 12, 2021 at 11:54:16 (UTC).
See https://pubs.acs.org/sharingguidelines for options on how to legitimately share published articles.

 © 2013 American Chemical Society dx.doi.org/10.1021/ja402150q | J. Am. Chem. Soc. 2013, 135, 7992−8000

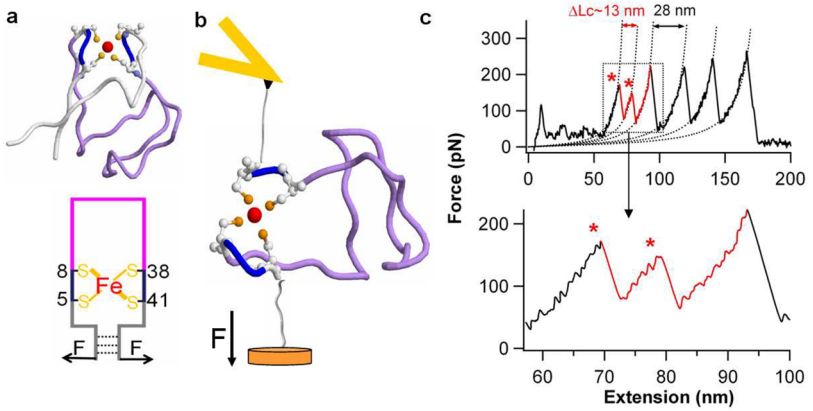


Figure 1. Investigation of the mechanical rupture of the $Fe(SCys)_4$ center in rubredoxin by single molecule AFM. (a) Three dimensional structure of wt rubredoxin (PDB: 1BRF).[33] The $Fe(SCys)_4$ center is shown in ball and stick representation where the ferric ion (in red) is coordinated to four cysteinyl sulfur atoms (in yellow). The two iron chelating loops C5XXC8 and C38XXC41 are colored in blue. Residues 8−41 (in pink) are sequestered by the iron center and will not be subject to the stretching force until the iron center has ruptured. The bottom panel shows a simplified schematic of the rubredoxin structure. (b) Schematic of the mechanical rupture of the $Fe(SCys)_4$ center by AFM. In this schematic, the $Fe(SCys)_4$ center is directly subject to the stretching force after residues 1−5 and 41−53 have been ruptured and extended. (c) Typical mechanical rupture events of the $Fe(SCys)_4$ center in wt rubredoxin. The force−extension curve is from the stretching of polyprotein chimera $(wt\text{-}RD\text{-}I27)_n$. It appears that rupture of the $Fe(SCys)_4$ center occurs in one step, as shown in the enlarged figure of the two rupture events at the bottom, resulting in a single force peak and a length increment of ΔLc ~13 nm. The force peaks with ΔLc ~28 nm are from the unfolding of the fused fingerprint protein domain I27.

MATERIALS AND METHODS

Protein Engineering. The gene encoding the rubredoxin variant with a β-hairpin fragment inserted in the C38XXC41 metal ion binding loop was constructed as follows. First, an oligodeoxyribonucleotide encoding the second β hairpin of GB1 (15 aa EWTYDDATKTFIVTE plus two 2 aa LG at each end that result from the restriction site) with an additional *Ava*I restriction site at the N and C termini was generated by standard polymerase chain reaction (PCR) methods with the GB1 gene as the template. The resulting gene was digested with the enzyme *Ava*I to produce the insert for subsequent ligation into the rubredoxin expression vector pQE80L, which carries an N-terminal His_6-purification tag. Standard site-directed mutagenesis methods were used to introduce an *Ava*I restriction site (CTC GGG), which replaces the codons CCC ATC that encode residues Pro39 and Ile40 (the residues between Cys38 and Cys41). DNA oligos encoding the β-hairpin fragment were then inserted into the rubredoxin gene between the Cys38 and Cys41 through the *Ava*I site. This construct introduces 19 residues (15 aa for the hairpin and 4 aa from the two *Ava*I sites) in the bicysteine loop to produce the rubredoxin loop extension variant with the sequence AKWVCKICGYIYDEDAGDPDNGISPGTKFEELPDDWVC*LGEW-TYDDATKTFIVTELG*CGAPKSEFEKLED (italics represent the inserted loop sequence).

For the expression of rubredoxin with an I27 domain as a fingerprint region for single molecule atomic force microscopy (AFM) studies, the gene encoding Cys-wt-RD-I27-Cys was used as the template for construction of the loop insertion variant using methods similar to those described above. In addition, the template possesses N- and C-terminal cysteinyl residues to facilitate the further construction of polyproteins by means of maleimide−thiol chemistry.[11,26] The DNA sequences were confirmed by direct DNA sequencing at the NAPS of University of British Columbia.

All proteins used in this work were overexpressed in *Escherichia coli* strain DH5α (Qiagen, Valencia, CA) and purified by Co^{2+}-affinity chromatography using TALON His-tag purification resins (Clontech, Mountain View, CA). The protein solution was exchanged into Tris buffer (pH 8.5, 10 mM) by centrifugal ultrafiltration (Amicon 3K MWCO filter, Millipore, Billerica, MA). Zn-substituted rubredoxin produced during expression of both RDβ2 and the RDβ2-I27 chimera was removed by ion-exchange chromatography using a mono Q 5/50 GL column (GE Healthcare Bioscience, Pittsburgh, PA). Polyproteins $(RD\beta2\text{-}I27)_n$, were prepared by a maleimide−thiol coupling reaction in which the monomer chimera protein was reacted with $BM(PEO)_3$ (1,8-bis (maleimido)triethylene glycol, Molecular Biosciences, Boulder, CO) as described previously.[26]

Single Molecule AFM. Single molecule AFM experiments were performed with a custom-built atomic force microscope as reported.[27] Prior to each experiment, the spring constant (~40 pN/nm) of each MLCT Si_3N_4 cantilever (Bruker, Camrillo, CA) was calibrated in solution using the equipartition theorem. In a typical experiment, the polyprotein $(RD\beta\text{-}I27)_n$ (2 μL, 2 mg/mL) was deposited onto a clean glass coverslip covered by Tris buffer (~50 μL, pH 7.4, 100 mM). The protein was allowed to absorb onto the coverslip for ~5 min before the AFM experiment. The experiments were carried out at a pulling speed of 400 nm/s unless otherwise indicated.

Monte Carlo Simulations. The mechanical rupture of single ferric-thiolate bond and the concurrent rupture of multiple ferric-thiolate bonds formed by the coordinated ferric ion and the C41XXC38 bicysteine ligand pair can both be modeled as a two-state dissociation process with a force-dependent rate constant:

$$\alpha_{(F)} = \alpha_0 \exp(F\Delta x_u/k_BT)$$

where $\alpha_{(F)}$ is the rate constant for dissociation under a stretching force F, α_0 is the rate constant for spontaneous dissociation in the absence of force, Δx_u is the distance between the bound and transition states, T is the absolute temperature, and k_B is the Boltzmann constant. The rate constant for dissociation at zero force, α_0, and Δx_u were estimated by Monte Carlo simulations as described previously.[28]

NMR Experiments. $^1H/^{15}N$ heteronuclear single-quantum coherence (HSQC) spectra were recorded on a Bruker Avance-500 FT NMR spectrometer operating at a ^1H frequency of 500 MHz using a standard pulse sequence. Spectra were zero-filled to give a final matrix of 2048 × 256 data points and apodized with a 90° shifted sine-bell window function in both dimensions. ^1H and ^{15}N chemical shifts were calibrated against the ^1H shift of sodium 2,2-dimethyl-2-silapentane-5-sulfonate.

Cyclic Voltammetry. Cyclic voltammetry (CV) experiments were carried out with an Autolab PGSTAT12 potentiostat-galvanostat (Eco Chemie, The Netherlands) with an edge-plane pyrolytic carbon working electrode (PGE). The PGE was polished with an alumina slurry and then sonicated in deionized water for 30 s before use. Typically, protein solution (2 μL, 2 mM) was spread onto the surface of the PGE with a microsyringe and then covered with a semipermeable membrane. A saturated calomel (SCE) electrode

dx.doi.org/10.1021/ja402150q | J. Am. Chem. Soc. 2013, 135, 7992−8000

(Radiometer, France) and platinum wire were used as the reference and counter electrodes, respectively. All experiments were carried out in sodium phosphate buffer (pH 7.0, 200 mM).

UV−Visible Absorption Spectroscopy Experiments. The electronic absorption spectra of wild-type (wt) and variant RDβ2 were recorded in Tris buffer (10 mM, pH 8.5) with a NanoDrop model ND-1000 spectrophotometer at room temperature. The protein concentration was ∼0.5 mM as determined from the absorbance of the solution at 495 nm (ε = 9.22 mM^{-1} cm^{-1}).[29]

Circular Dichroism Spectroscopy Experiments. Circular dichroism (CD) spectra were recorded with a Jasco Model J810 spectropolarimeter using a quartz cuvette with a path length of 0.2 cm. For these measurements, protein samples with concentration of ∼1 mM were used. For the far-UV CD measurements, the same protein samples were diluted with distilled water to ∼10 μM for measurements.

RESULTS

Construction and Use of a Loop Elongation Variant of Rubredoxin for Detection of Single-Bond Rupture Events. We chose the simplest iron−sulfur protein *Pyrococcus furiosus* rubredoxin with a $Fe(SCys)_4$ center as our model system to study the mechanical rupture mechanism of the metal center. As a simple electron transfer protein with only 53 residues, rubredoxin contains two classic CXXC loops (C5XXC8 and C38XXC41) that bind a ferric ion and form four ferric-thiolate bonds (Figure 1a).[29−31] Recently, we showed that these highly covalent ferric-thiolate bonds in rubredoxin can be mechanically activated and ruptured by single molecule AFM (Figure 1b). Our previous AFM results showed that the mechanical unfolding of rubredoxin follows a two-step process.[11,32] Residues (1−5 and 41−53) outside the metal center are unraveled first by the stretching force, while the residues sequestered by the metal center (residues 5−41) are shielded from the stretching force. Further stretching leads to the mechanical rupture of the ferric-thiolate bonds, disruption of the $Fe(SCys)_4$ center, and complete unfolding of rubredoxin. Mechanical rupture of the iron center appears to involve concurrent rupture of multiple ferric-thiolate bonds, as the rupture of the metal center led to a one-step extension of the protein by ∼13 nm, which agrees well with the extension of residues 5−41(Figure 1c). However, the two chelating loops C5XXC8 and C38XXC41 are very short. If the mechanical rupture of $Fe(SCys)_4$ was to occur in a sequential fashion, the rupture of a single ferric-thiolate bond formed by Fe and C5 or C41 would lead to a length increment of 0.72 nm resulting from the extension of the two XX residues. This short length gain cannot be detected in a soft polymer chain by current single molecule AFM instruments. As a result, the mechanical rupture event observed in the force−extension curve may be dominated by the subsequent rupture event of the additional ferric-thiolate bond, and a sequential mechanical rupture process cannot be resolved.

To overcome this technical challenge and gain a detailed insight into the mechanical rupture mechanism of the iron center in rubredoxin, we designed a loop elongation variant of rubredoxin (RDβ2), in which a long loop is inserted into the C38XXC41 chelating loop. Insertion of a long loop into the CXXC chelating loop should permit any potential sequential mechanical rupture events to be captured unambiguously.

To construct the loop elongation rubredoxin variant RDβ2 while maintaining the structural and functional properties of wt rubredoxin, we inserted the second β hairpin of a small protein GB1 into the C38XXC41 chelation loop,[34] which is located in a largely unstructured region of rubredoxin. It is well-known that the second β hairpin of GB1 is only marginally stable in isolation and adopts ∼40% of nativelike β-hairpin structure at room temperature in water.[35,36] In the folded state, the N and C termini of this structural element are close to each other (0.4 nm apart). Thus, the insertion of this β hairpin into C38XXC41 should not affect the structure of rubredoxin or the iron center. In addition, since the hairpin is mechanically labile,[37] stretching this hairpin will not generate any observable force peaks but result in a contour length gain of ∼6.8 nm (19 aa × 0.36 nm/aa), which corresponds to the length of the 19 residue hairpin. Thus, this ∼6.8 nm length gain will provide an unambiguous signature for the sequential rupture of the $Fe(SCys)_4$ center and a measure of the mechanical stability of the Fe−Cys41 bond.

To evaluate the consequences of the β-hairpin insertion on the structure of the $Fe(SCys)_4$ center and the overall structure of the protein, we undertook spectroscopic characterizations of the variant protein RDβ2 (Figure 2a−d). The electronic absorption spectrum of RDβ2 exhibits maxima at 390, 495, and 570 nm resulting from ligand-to-metal charge-transfer transitions that are identical to those of oxidized, wt rubredoxin.[30,38] The reduction potential of RDβ2 is similar to that of wt rubredoxin. These results strongly suggest that the coordination environment of the $Fe(SCys)_4$ center is not affected by the

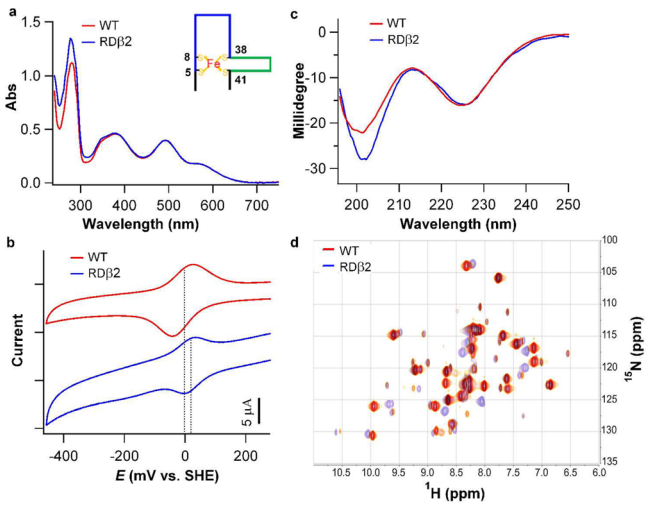


Figure 2. Iron center and overall three-dimensional structure are minimally perturbed in the loop insertion variant RDβ2 relative to the structure of the wt protein. (a) UV−visible spectrum of RDβ2 (in blue) exhibits the characteristic features of the wt protein (in red) and the same A_{484}/A_{380} ratio. Absorbance at 280 nm (A_{280}) of the variant is higher than that of wt rubredoxin due to the tyrosine residue in the inserted loop. The inset shows a simplified schematic of RDβ2, where the inserted loop is colored in green. (b) CV of wt rubredoxin and the RDβ2 variant. The reduction potential of RDβ2 (15 mV) shows slight shift compared with that of wt RD (−4 mV). (c) Far-UV CD spectrum of wt rubredoxin and the RDβ2 variant. The small change of the CD signal at ∼200 nm for the variant is probably attributable to disruption of the β turn upon insertion of the β hairpin. (d) Overlap of the HSQC spectra of RDβ2 and wt RD (Fe(III)). 58 signals from the wt RD spectrum (in red), which are not affected significantly by the paramagnetic ferric ion, were also observed in the RDβ2 spectrum (in blue). 54 out of 58 signals of RDβ2 appear at the same or slightly shifted (<0.5 ppm in ^{1}H) positions as wt rubredoxin, strongly suggesting that the backbone structure of RDβ2 is very similar to that of wt RD.

dx.doi.org/10.1021/ja402150q | J. Am. Chem. Soc. 2013, 135, 7992−8000

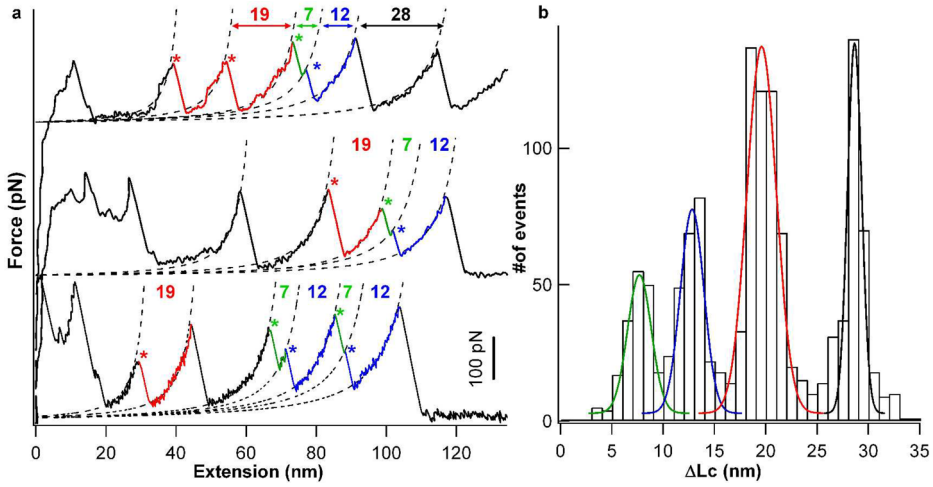


Figure 3. Mechanical unfolding experiments on rubredoxin loop variant RDβ2 demonstrate a complex rupture pattern of the Fe(SCys)$_4$ center. (a) Typical force−extension curves observed during stretching the polyprotein (RDβ2-I27)$_n$. In addition to the unfolding force peaks from the I27 domain (ΔLc ∼28 nm), three distinct rupture force peaks resulting from unfolding of the RDβ2 are observed. The dominant component (∼80%) is a single force peak (as indicated by red *) with a ΔLc value of 19 nm (colored in red). The remaining events (∼20%) involve two sequential force peaks with ΔLc values of 7 and 12 nm, respectively (colored in green and blue). (b) Histogram of the contour length increment of the unfolding experiments on the polyprotein (RDβ2-I27)$_n$ clearly shows the four different types of peak: the average ΔLc values for these four components are 7.2 ± 1.6 nm (n = 121), 12.3 ± 1.6 nm (n = 121), 19.1 ± 2.0 nm (n = 547), and 28.2 ± 1.0 nm (n = 327). The first three peaks result from the unfolding of RDβ2, and the fourth one results from the unfolding of I27 domains.

insertion of the β hairpin and that the iron center retains electron transfer properties similar to the wt protein.[29] In addition, the far-UV CD spectrum of RDβ2 is similar to that of wt rubredoxin, suggesting that the three-stranded antiparallel β-sheet structure remains largely intact. This conclusion is further supported by the ^{1}H/^{15}N HSQC experiments. In Figure 2d, 58 signals from the wt RD spectrum, which are not significantly affected by the paramagnetic ferric ion, were shown. All these signals were also observed in the spectrum of RDβ2, and 54 out of 58 signals appear at the same or slightly shifted (<0.5 ppm in ^{1}H) positions.[39] These results provide strong evidence that the structural and functional properties of rubredoxin are minimally perturbed by this loop insertion.

With this loop elongation variant, we are now able to distinguish whether the bonds between the ferric ion and the new bicysteine binding motif rupture in a concurrent or sequential fashion upon mechanical rupture. If the two ferric-thiolate bonds Fe−Cys38 and Fe−Cys41 rupture concurrently, the mechanical rupture of the Fe(SCys)$_4$ center should result in a single unfolding step with a contour length increment (ΔLc) of ∼18.7 nm (6.8 + 11.9 nm), which corresponds to the extension of the inserted β hairpin together with the residues sequestered between residues C5 and C41. In the case of a sequential mechanical rupture mechanism, two rupture events should be observed. The first event (ΔLc = 6.8 nm) corresponds to the extension of the inserted β hairpin, and the second event (ΔLc = 12 nm) corresponds to the extension of residues 5−38. Consequently, both the concurrent and sequential mechanisms for Fe−ligand bond rupture can be identified unambiguously from unique signatures in the force−extension curves.

Direct Observation of Multiple Pathways for Iron Release from the Fe(SCys)$_4$ Center of Rubredoxin. To monitor the mechanical rupture pathways of the Fe(SCys)$_4$ center in rubredoxin directly, we constructed a polyprotein chimera (RDβ2-I27)$_n$ for single molecule force spectroscopy measurements. This chimera incorporates the well-characterized I27 domain from the giant muscle protein titin to provide an unambiguous fingerprint for identification of single molecule stretching events.[40,41] The mechanical unfolding of the I27 domain is characterized by a ΔLc value of 28 nm and an unfolding force of ∼200 pN at a pulling speed of 400 nm/s.

Representative force−extension curves for this polyprotein chimera (RDβ2-I27)$_n$ are shown in Figure 3a. The unfolding events with a ΔLc value of 28 nm can be assigned readily to the unfolding of the I27 domains while the other unfolding events can be assigned to the unfolding of RDβ2 domains. The complete unfolding of RDβ2 leads to a contour length increment ΔLc value of ∼19 nm. In the force−extension curves, the unfolding events of RDβ2 display multiple appearances: some unfolding events display a single unfolding step with a ΔLc value of ∼19 nm while others display two unfolding steps with the sum of ΔLc1 and ΔLc2 being 19 nm. In most of the two-step unfolding cases, the first step leads to a ΔLc value of ∼7 nm followed by a second step of a ΔLc value of ∼12 nm. In rare cases, the sequence of the two steps reverses so that the first peak exhibits a ΔLc value of ∼12 nm that is followed by an unfolding step with a ΔLc value of ∼7 nm (Figure S1, Supporting Information). The histogram of ΔLc values (Figure 3b) clearly exhibits three dominant peaks for RDβ2 with an average ΔLc1 value of 7.2 ± 1.6 nm (n = 121), a ΔLc2 value of 12.3 ± 1.6 nm (n = 121), and a ΔLc3 value of 19.1 ± 2.0 nm (n = 547). The fourth peak, with an average of 28.2 ± 1.0 nm (n = 327), corresponds to the ΔLc of the unfolding of I27 domains.

The observation of multiple unfolding patterns for RDβ2 demonstrates clearly that the mechanical rupture of the Fe(SCys)$_4$ center in rubredoxin occurs through multiple pathways, including both single-step rupture as well as sequential rupture. This finding establishes the complexity of the mechanical rupture of the Fe(SCys)$_4$ center in rubredoxin and demonstrates the rich information about the mechanical rupture mechanism of the metal center that cannot be discerned from ensemble studies.

dx.doi.org/10.1021/ja402150q | J. Am. Chem. Soc. 2013, 135, 7992−8000

Concurrent Rupture of Multiple Ferric-Thiolate Bonds in the Fe(SCys)$_4$ Center Is the Dominant Mechanism for Iron Release. From typical sawtoothlike force−extension traces of the polyprotein chimera (RDβ2-I27)$_n$, we observed that a large population of RDβ2 (~81%) unfolds in a single step that results in unfolding events of a ΔLc value of ~19 nm (Figure 4a,b). The average of the measured ΔLc (19.1 nm (n = 547)) is in excellent agreement with the expected contour length increment that should result from the extension of residues sequestered by the metal center (residues 5−38) as well as the inserted β hairpin (11.6 + 6.9 = 18.7 nm), suggesting that the two ferric-thiolate bonds from the C38XXC41 chelating loop must have been ruptured concurrently by the applied stretching force during the mechanical rupture (Figure 4a). This result is strong evidence for a concurrent mechanical rupture process for the Fe(SCys)$_4$ center, despite the insertion of the 19 residue long β hairpin. The average force required to rupture the two ferric-thiolate bonds simultaneously is 194 ± 92 pN (n = 547) (Figure 4c). To confirm that the single-step unfolding is not an artifact of limited time resolution, we carried out the single molecule AFM experiments at a higher data sampling rate, and a represented curve is shown in Figure 4b (bottom trace). The force-relaxation part of the curve (as indicated by the blue crosses) can be fitted with a perfect linear fit with a slope that is equal to the spring constant of the cantilever, and no kink or plateau was detected. This result strongly indicated that the unfolding step remains a single step at a sampling frequency of 50 kHz, suggesting that the mechanical rupture of the Fe(SCys)$_4$ center occurs simultaneously within a time window of 20 μs. This result highlights the cooperativity of the Fe(SCys)$_4$ center in rubredoxin as observed previously in ensemble studies (i.e., first-order kinetics for the dissociation of the Fe(SCys)$_4$ center).[21,23,42]

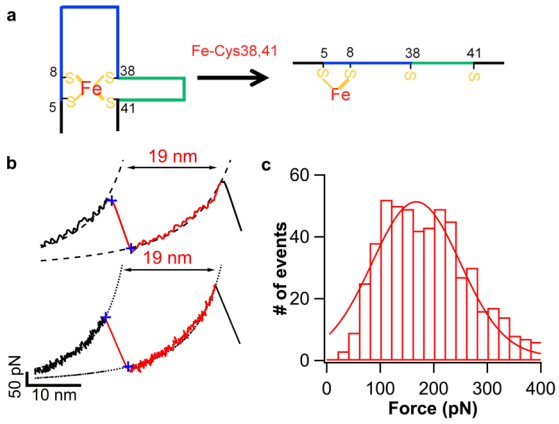


Figure 4. Concurrent mechanism for mechanical disruption of the rubredoxin Fe(SCys)$_4$ center. (a) Schematic of the concurrent rupture pathway of the Fe(SCys)$_4$ center in RDβ2. Upon stretching, two ferric-thiolate bonds (Fe−S_{Cys38} and Fe−S_{Cys41}) ruptured concurrently, leading to a single force peak. (b) Detailed view of the single-step rupture event of the Fe(SCys)$_4$ center at two sampling rates. Top trace, 1 kHz; bottom trace, 50 kHz. It is clear that the rupture event with a ΔLc value of ~19 nm is a single step. (c) Rupture force histogram for the concurrent rupture of multiple ferric-thiolate bonds in the Fe(SCys)$_4$ center. The average rupture force is 194 ± 92 pN (n = 547).

Sequential Mechanism for Iron Release from the Fe(SCys)$_4$ Center in Rubredoxin and Measurement of the Bond Strengths of Individual Ferric-Thiolate Bonds. In addition to the dominant concurrent mechanical rupture, we also observed that ~20% of RDβ2 is ruptured in a sequential fashion by the applied stretching force. As shown in Figure 5a,b,

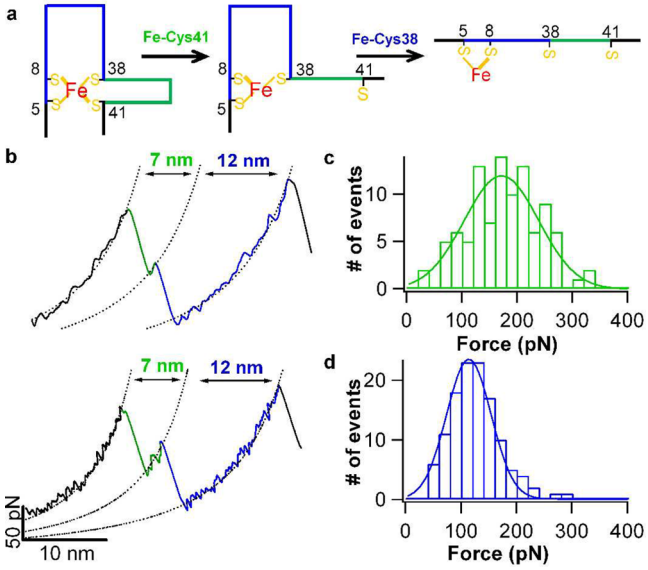


Figure 5. Sequential mechanism for disruption of the rubredoxin Fe(SCys)$_4$ center. (a) Schematic of a sequential rupture pathway of the Fe(SCys)$_4$ center in RDβ2 where the two ferric-thiolate bonds (Fe−Cys38 and Fe−Cys41) rupture sequentially. The Fe−Cys41 bond ruptures first, leading to an intermediate Fe(SCys)$_3$ and the extension of the inserted β hairpin (color in green). Then, the rupture of the Fe−Cys38 bond leads to the complete unfolding of rubredoxin and extension of the sequestered residues (color in blue). (b) Detailed view of the sequential rupture of the Fe(SCys)$_4$ center in RDβ2. (c) Rupture force histogram of the ferric-thiolate bond Fe−Cys41. The average force is 176 ± 63 pN (n = 99). (d) Rupture force histogram of the ferric-thiolate bond Fe−Cys38. The average force is 127 ± 48 pN (n = 99).

the mechanical rupture of RDβ2 domains resulted in pairs of unfolding force peaks. The first peak (ΔLc ~ 7 nm (colored in green, 7.2 ± 1.6 nm)) occurs at a slightly elevated force relative to the second peak (ΔLc ~ 12 nm (colored in blue, 12.3 ± 1.6 nm)) (Figure S2a, Supporting Information). The ΔLc of the first peak agrees well with that for the extension of the inserted loop initiated by the rupture of the Fe−Cys41 bond (0.36 nm/aa × 19 aa = 6.9 nm) while the value for the second peak agrees well with the value for the complete rupture of the partially disrupted Fe(SCys)$_3$ center (34 aa × 0.36 nm/aa − 0.6 nm = 11.6 nm, where 0.6 nm is the distance between C5 and C38 in the structure of rubredoxin). These results strongly suggest that the RDβ2 domains rupture in a stepwise, sequential fashion such that the Fe−Cys41 and Fe−Cys38 bonds rupture sequentially.

Moreover, from the pair of force peaks resulting from these sequential rupture events, we can attribute the rupture force value of each step to the mechanical strength of a single ferric-thiolate bond (Fe−Cys41 or Fe−Cys38). The average rupture force of the first peak (176 ± 62 pN (n = 99, Figure 5c)) corresponds to the mechanical strength of the Fe−Cys41 bond while the rupture force of the second peak (127 ± 48 pN (n = 99, Figure 5d)) corresponds to the strength of the Fe−Cys38 bond. From the force−extension curve as well as the rupture force histogram, it is evident that the mechanical strength of the Fe−Cys41 bond is greater than that of the Fe−Cys38 bond.

dx.doi.org/10.1021/ja402150q | J. Am. Chem. Soc. 2013, 135, 7992−8000

This observation is consistent with the bond lengths of the two distinct ferric-thiolate bonds insofar as the shorter bond (Fe−Cys41) is stronger than the longer bond (Fe−Cys38). However, it is also important to note that the rupture force measured for the Fe−Cys38 bond may not represent the mechanical stability of the "original" Fe−Cys38 bond, because the mechanical rupture of the Fe−Cys41 bond will convert the FeS center from a four-coordinate species $Fe(SCys)_4$ to a three-coordinate species $Fe(SCys)_3$. In addition, the disruption of the C38XXC41 loop and solvent exposure could also weaken the Fe−Cys38 bond and facilitate the rupture of the Fe−Cys38 bond, a fashion similar to the cooperative binding of O_2 to deoxyhemoglobin (binding of one O_2 to deoxyhemoglobin makes binding of the second easier). Determining the "true" mechanical strength of the Fe−Cys38 bond in its native environment remains an experimental challenge.

Remarkably, we also detected two-step rupture events in which the order of Fe−Cys bond disruption was reversed so that the rupture event with a ΔLc value of 12 nm occurred first, followed by the rupture event with a ΔLc value of 7 nm (Figure S1, Supporting Information, n = 22). This sequence of rupture events suggests that the rupture of the $Fe(SCys)_4$ center can also be initiated from the side of the C5XXC8 chelating loop, indicating that the mechanical rupture of the $Fe(SCys)_4$ center in rubredoxin is stochastic in nature and can be initiated from either CXXC chelating loop.[43]

Having observed multiple mechanical rupture pathways for disruption of the rubredoxin active site, we carried out pulling experiments at different pulling velocities to characterize bond rupture kinetics (Figure S2b, Supporting Information). As expected, the rupture forces were observed to increase with the increase of the pulling velocity. Using well-established Monte Carlo simulation protocols,[28] we estimated the spontaneous dissociation rate and the distance between the bound state and the mechanical rupture transition state. For the concurrent rupture pathway, the rate constant for spontaneous dissociation at zero force (α_0) is 0.17 s^{-1}, and the distance between the bound state and the mechanical rupture transition state, Δx_u, is 0.11 nm. These values are quite similar to those observed for wt RD (0.15 s^{-1} and 0.11 nm).[11] In contrast, the kinetics for single-bond rupture events is significantly different. The Δx_u value is 0.13 nm for Fe−Cys41 and Fe−Cys38 with α_0 values of 0.21 and 1.4 s^{-1}, respectively. The difference in the kinetics data of the two distinct mechanical rupture pathways also demonstrates that these two rupture mechanisms are different in nature. Moreover, in our pulling speed dependence experiments, the relative occurrence frequency of the two rupture mechanisms does not show obvious dependence on the pulling speed.

It is interesting to note that, in the sequential mechanical rupture pathway, the mechanically stronger bond Fe−Cys41, which shows a smaller α_0, ruptures first followed by the mechanical rupture of the weaker bond Fe−Cys38, which displays a larger α_0. This result reveals an abnormal mechanical hierarchy for the two Fe-thiolate bonds. It is important to point out that this abnormal mechanical hierarchy is due to the pulling geometry used in our experiments. In this pulling geometry, the Fe−Cys41bond will be subject to the stretching force directly and likely experience greater force than the Fe−Cys38 bond. In contrast, the Fe−Cys38 bond will be subject to the stretching force directly only after the Fe−Cys41 bond has ruptured. As such, the rupture of Fe−Cys38 will likely not occur before Fe−Cys41 has ruptured. Hence, the Fe−Cys41 bond can protect the mechanical integrity of the Fe−Cys38 bond by means of a gating mechanism. A similar gating mechanism has been reported for both designed, artificial proteins[34] and naturally occurring proteins, such as titin kinase in muscles.[44,45]

DISCUSSION

Stochastic Nature of Iron Release from the $Fe(SCys)_4$ Center of Rubredoxin. Metal centers with multiple metal−ligand bonds are a common feature in metalloproteins.[12,13,30] The loss of metal ions in metalloproteins can have significant biological consequences, and understanding the rupture mechanism of such metal centers in metalloproteins is thus of great importance.[12,14−17] The release of metal ions from metalloproteins involves the dissociation of multiple metal−ligand bonds, and detailed rupture pathways have been difficult to elucidate with classical ensemble techniques because such methods are typically unable to detect short-lived and/or less populated intermediate species in which just one or two metal−ligand bonds have been ruptured. The single molecule force spectroscopy techniques used here provide the first unambiguous experimental evidence that the mechanical rupture of even a simple iron center such as that in the iron−sulfur protein rubredoxin is stochastic and follows multiple, complex pathways that include concurrent rupture of multiple ferric-thiolate bonds as well as sequential rupture of ferric-thiolate bonds that lead to the formation of intermediate species.

On the basis of these results, we propose the following stochastic mechanism for mechanical rupture of the $Fe(SCys)_4$ center in rubredoxin (Figure 6). Mechanical rupture can initiate from either the C5XXC8 side or the C38XXC41 side of the metal center (C5XXC8 or C38XXC41), and the subsequent rupture from either side involves both concurrent and sequential rupture mechanisms. Although this model is based primarily on results obtained with RDβ2, we expect that the

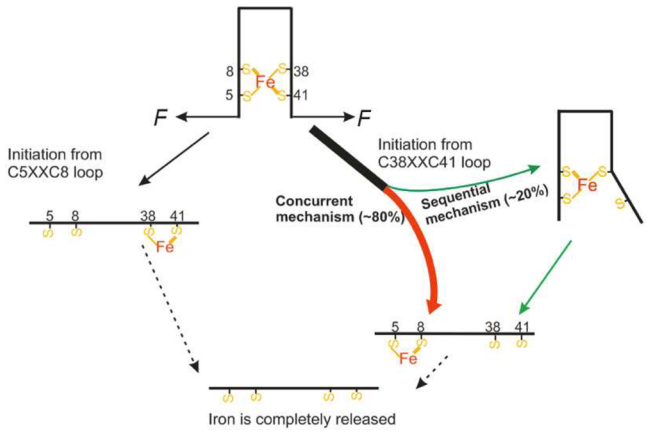


Figure 6. Stochastic mechanical disruption of the rubredoxin $Fe(SCys)_4$ center derived from single molecule force spectroscopy experiments. The rupture of $Fe(SCys)_4$ can be initiated at either CXXC loop. For the pathway initiated at the C38XXC41loop, 80% of rupture events occur in a single step in which two ferric-thiolate bonds rupture concurrently. In addition, 20% of Fe−Cys bond-rupture events occur in a sequential fashion in which the Fe−Cys41 bond ruptures first followed by the rupture of the Fe−Cys38 bond. For the pathway initiated through the C5XXC8 loop, it is very likely both concurrent and sequential rupture processes occur in a manner similar to that observed for the C38XXC41 loop. Dashed lines indicate the processes in which iron is completely released from rubredoxin.

dx.doi.org/10.1021/ja402150q | J. Am. Chem. Soc. 2013, 135, 7992−8000

mechanical rupture of the metal center initiated from the C5XXC8 loop will follow a similar mechanism. It is important to note that the pathway for mechanical rupture of the (Fe–Cys)$_4$ center in wt rubredoxin is likely to be more complex because it should involve a combination of rupture events from both CXXC chelation loops. For example, it is possible that the mechanical rupture of the wt rubredoxin starts from the breaking of the Fe–Cys5 bond followed by the concurrent rupture of the C38XXC41 chelation loop.

Concurrent versus Sequential Bond Rupture. With the length increment as an unambiguous fingerprint, we clearly identified the coexistence of the concurrent and sequential mechanical rupture pathways for the Fe(SCys)$_4$ center in rubredoxin. The observation of concurrent bond rupture of multiple ferric-thiolate bonds even in the presence of an inserted long β hairpin clearly highlights the cooperative character of the Fe(SCys)$_4$ center disruption, a feature that has been proposed on the basis of ensemble measurements.[42]

On the other hand, the discovery of the sequential rupture pathway sheds new light on the Fe(SCys)$_4$ center in rubredoxin. Direct detection of partially or completely unfolded metalloprotein with metal ion still bound to the protein could in principle be identified by NMR spectroscopy.[16,46,47] However, a partially ruptured metal center that should occur as an intermediate during the disruption of metal centers has not been observed for rubredoxin. The sequential rupture pathway demonstrated in the present study clearly indicates that the intermediate states such as Fe(SCys)$_3$ are kinetically stable and can exist in aqueous solutions of rubredoxin. The formation of Fe(SCys)$_3$ can result from cleavage of the Fe–Cys41 bond or the Fe–Cys5 bond. To the best of our knowledge, this is the first experimental evidence that an intermediate iron center can occur during the release of iron from rubredoxin. This finding implies that the Fe(SCys)$_4$ center in rubredoxin can be more dynamic than previously believed. However, it remains unknown whether such an intermediate metal center could have any functional roles. The existence of a stable metal center intermediate also supports the hypothesis that iron priming is an important step in the folding of rubredoxin and that incorporation of iron into rubredoxin involves the sequential formation of ferric-thiolate bonds.[19,48]

Why Is Iron Release Stochastic. Although rubredoxin is the simplest iron–sulfur protein, the mechanical rupture of Fe(SCys)$_4$ center exhibits a complex mechanism. Understanding how a stretching force ruptures the Fe(SCys)$_4$ center in rubredoxin will provide fundamental insight that will be essential to understanding the mechanism of iron release from more complex iron–sulfur proteins. The Fe(SCys)$_4$ center in rubredoxin is a five atom, four bond system in which the ferric ion is at the center of a pseudotetrahedron and is bonded to four sulfur atoms provided by the four chelating cysteinyl residues. Following the unraveling and extension of residues 1–5 and 41–53, the Fe(SCys)$_4$ center of rubredoxin is subject to the mechanical stretching force directly through residues C5 and C41. To rupture the Fe(SCys)$_4$ center mechanically, at least two ferric-thiolate bonds from the same side of the CXXC chelation loop must be ruptured.

Compared with classic chemical or thermal dissociation processes that impose a global perturbation on the metal center, the mechanical rupture process stretches the metal center along a well-defined reaction coordinate that is set by the applied force. Upon stretching, the two outer ferric-thiolate bonds (Cys5 and Cys41) are likely to be subject to greater force at the beginning of the process than are the two inner bonds formed by Cys8 and Cys38. Thus, the greater mechanistic resolution provided by single molecule atomic force spectroscopy has allowed us to observe the sequential mechanism of iron release from the active site of rubredoxin that could not be detected by conventional methods. Nevertheless, the dominant pathway for iron release is the concerted rupture of two ferric-thiolate bonds, an observation that highlights the cooperative nature of the iron dissociation process in rubredoxin. We interpret this finding as an indication that the stretching force propagates to the entire metal center through the bonding network as predicted for the propagation of the applied force through an entire protein upon stretching.[49−52] We propose that propagation of the stretching force through the active site in this manner is responsible for the concurrent disruption of multiple ferric-thiolate bonds.

However, the detailed molecular mechanism underlying the concurrent rupture process of the iron center in rubredoxin remains to be elucidated. Combined use of molecular dynamics simulation with quantum mechanical description of the iron center provides one plausible means of addressing this issue.[7,53]

Single Molecule AFM Experiments Enable the Direct Measurement of the Mechanical Strength of a Single Fe-Thiolate Bond in a Metalloprotein. In addition to discovering and partially characterizing the mechanistic pathways for iron release from rubredoxin, this study provides quantitative characterization of the mechanical strength of individual ferric-thiolate bonds in rubredoxin and suggest that these nominally identical metal–ligand bonds may be energetically inequivalent. Although X-ray crystallographic structure determination has established that the Fe–C41 bond is shorter than the Fe–C38 bond,[36] the physical properties of these minimally different chemical bonds have been challenging to discern. To the best of our knowledge, no comparison of the mechanical strength of nearly identical chemical bonds involved in metal ion binding at the active site of a metalloprotein or in a biomimetic metal cluster has been reported.[1,2] Our characterization of loop insertion variant of rubredoxin has determined that the bond strengths of Fe–Cys41 (in a (Fe(SCys)$_4$ species) and Fe–Cys38 (in a Fe(SCys)$_3$ species) in this protein are ∼170 and ∼130 pN, respectively, a result that agrees well with our previous indirect measurements of rubredoxin variants in which the coordinating cysteinyl residues were replaced with histidinyl residues.[11,26] We expect that this strategy can be applied to other metalloproteins to resolve small energetic differences of chemically identical metal–ligand bonds of inequivalent length.

■ CONCLUSIONS

In this study, we have combined single molecule force spectroscopy and protein engineering techniques to investigate the mechanical rupture mechanism of the iron–sulfur center Fe(SCys)$_4$ of the simplest iron–sulfur protein, rubredoxin, at the single molecule level. Our results reveal that the mechanical rupture of this simplest iron center is stochastic and can be initiated from either the C38XXC41 chelation loop or the C5XXC8 loop. The subsequent rupture of the Fe(SCys)$_4$ center follows multiple, complex pathways that include concurrent rupture of multiple ferric-thiolate bonds as well as sequential rupture of ferric-thiolate bonds that leads to the formation of intermediate iron–sulfur species. Our results provide the first unambiguous experimental description of the mechanical disruption pathway of a metal center in its native

protein environment in aqueous solution and reveal the unexpected complexity of the mechanical rupture mechanism of the simplest iron sulfur protein. Our study also demonstrates the unique application of single molecule force spectroscopy techniques in elucidating detailed mechanistic insight into the mechanical rupture mechanism of metal centers in a broad range of metalloproteins.

■ ASSOCIATED CONTENT

Supporting Information

Representative force−extension curve for the rupture of the FeS4 center initialed through the C5XXC8 loop; ferric-thiolate bond strength and kinetics. This material is available free of charge via the Internet at http://pubs.acs.org.

■ AUTHOR INFORMATION

Corresponding Author

Hongbin@chem.ubc.ca

Notes

The authors declare no competing financial interest.

■ ACKNOWLEDGMENTS

We thank Professor Strauss for stimulating discussion. This work was supported by the Natural Sciences and Engineering Research Council of Canada (H.L.) and Canada Foundation for Innovation and Canada Research Chairs program (H.L. and A.G.M.).

■ REFERENCES

(1) Grandbois, M.; Beyer, M.; Rief, M.; Clausen-Schaumann, H.; Gaub, H. E. *Science* **1999**, *283*, 1727.

(2) Beyer, M. K.; Clausen-Schaumann, H. *Chem. Rev.* **2005**, *105*, 2921.

(3) Davis, D. A.; Hamilton, A.; Yang, J.; Cremar, L. D.; Van Gough, D.; Potisek, S. L.; Ong, M. T.; Braun, P. V.; Martinez, T. J.; White, S. R.; Moore, J. S.; Sottos, N. R. *Nature* **2009**, *459*, 68.

(4) Black, A. L.; Lenhardt, J. M.; Craig, S. L. *J. Mater. Chem.* **2011**, *21*, 1655.

(5) Hickenboth, C. R.; Moore, J. S.; White, S. R.; Sottos, N. R.; Baudry, J.; Wilson, S. R. *Nature* **2007**, *446*, 423.

(6) Garcia-Manyes, S.; Liang, J.; Szoszkiewicz, R.; Kuo, T. L.; Fernandez, J. M. *Nat. Chem.* **2009**, *1*, 236.

(7) Aktah, D.; Frank, I. *J. Am. Chem. Soc.* **2002**, *124*, 3402.

(8) Evans, E. *Annu. Rev. Biophys. Biomol. Struct.* **2001**, *30*, 105.

(9) Schmidt, S. W.; Filippov, P.; Kersch, A.; Beyer, M. K.; Clausen-Schaumann, H. *ACS Nano* **2012**, *6*, 1314.

(10) Alegre-Cebollada, J.; Kosuri, P.; Rivas-Pardo, J. A.; Fernandez, J. M. *Nat. Chem.* **2011**, *3*, 882.

(11) Zheng, P.; Li, H. *J. Am. Chem. Soc.* **2011**, *133*, 6791.

(12) Lippard, S. J.; Berg, J. M. *Principles of Bioinorganic Chemistry*; University Science Books: Mill Valley, CA, 1994.

(13) Holm, R. H.; Kennepohl, P.; Solomon, E. I. *Chem. Rev.* **1996**, *96*, 2239.

(14) Dudev, T.; Lim, C. *Annu. Rev. Biophys.* **2008**, *37*, 97.

(15) Wilson, C. J.; Apiyo, D.; Wittung-Stafshede, P. *Q. Rev. Biophys.* **2004**, *37*, 285.

(16) Wittung-Stafshede, P. *Acc. Chem. Res.* **2002**, *35*, 201.

(17) Loh, S. N. *Metallomics* **2010**, *2*, 442.

(18) Winkler, J. R.; WittungStafshede, P.; Leckner, J.; Malmstrom, B. G.; Gray, H. B. *Proc. Natl. Acad. Sci. U.S.A.* **1997**, *94*, 4246.

(19) Morleo, A.; Bonomi, F.; Iametti, S.; Huang, V. W.; Kurtz, D. M. *Biochemistry* **2010**, *49*, 6627.

(20) Dukes, G. R.; Holm, R. H. *J. Am. Chem. Soc.* **1975**, *97*, 528.

(21) Cavagnero, S.; Debe, D. A.; Zhou, Z. H.; Adams, M. W. W.; Chan, S. I. *Biochemistry* **1998**, *37*, 3369.

(22) Shimazaki, Y.; Takani, M.; Yamauchi, O. *Dalton Trans.* **2009**, 7854.

(23) Henriques, B. J.; Saraiva, L. M.; Gomes, C. M. *Biochem. Biophys. Res. Commun.* **2005**, *333*, 839.

(24) Leal, S. S.; Teixeira, M.; Gomes, C. M. *J. Biol. Inorg. Chem.* **2004**, *9*, 987.

(25) Crack, J. C.; den Hengst, C. D.; Jakimowicz, P.; Subramanian, S.; Johnson, M. K.; Buttner, M. J.; Thomson, A. J.; Le Brun, N. E. *Biochemistry* **2009**, *48*, 12252.

(26) Zheng, P.; Cao, Y.; Li, H. *Langmuir* **2011**, *27*, 5713.

(27) Carrion-Vazquez, M.; Oberhauser, A. F.; Fisher, T. E.; Marszalek, P. E.; Li, H.; Fernandez, J. M. *Prog. Biophys. Mol. Biol.* **2000**, *74*, 63.

(28) Rief, M.; Fernandez, J. M.; Gaub, H. E. *Phys. Rev. Lett.* **1998**, *81*, 4764.

(29) Blake, P. R.; Park, J. B.; Bryant, F. O.; Aono, S.; Magnuson, J. K.; Eccleston, E.; Howard, J. B.; Summers, M. F.; Adams, M. W. *Biochemistry* **1991**, *30*, 10885.

(30) Solomon, E. I.; Gorelsky, S. I.; Dey, A. *J. Comput. Chem.* **2006**, *27*, 1415.

(31) Johnson, D. C.; Dean, D. R.; Smith, A. D.; Johnson, M. K. *Annu. Rev. Biochem.* **2005**, *74*, 247.

(32) Zheng, P.; Takayama, S.-i. J.; Mauk, A. G.; Li, H. *J. Am. Chem. Soc.* **2012**, *134*, 4124.

(33) Bau, R.; Rees, D. C.; Kurtz, D. M., Jr.; Scott, R. A.; Huang, H.; Adams, M. W. W.; Eidsness, M. K. *J. Biol. Inorg. Chem.* **1998**, *3*, 484.

(34) Gronenborn, A. M.; Filpula, D. R.; Essig, N. Z.; Achari, A.; Whitlow, M.; Wingfield, P. T.; Clore, G. M. *Science* **1991**, *253*, 657.

(35) Blanco, F. J.; Rivas, G.; Serrano, L. *Nat. Struct. Biol.* **1994**, *1*, 584.

(36) Day, M. W.; Hsu, B. T.; Joshuator, L.; Park, J. B.; Zhou, Z. H.; Adams, M. W. W.; Rees, D. C. *Protein Sci.* **1992**, *1*, 1494.

(37) Cao, Y.; Li, H. *Nat. Mater.* **2007**, *6*, 109 (Our previous single molecule AFM experiments on GB1 showed that the mechanical unfolding of GB1 is two state, and no mechanical unfolding intermediate state that corresponds to the unraveling of the second β hairpin was observed. These results indicated that the second β hairpin of GB1 is mechanically labile and does not exhibit any measurable mechanical stability. Thus, all the mechanical force should be stored entirely within the Fe−S bonds, and the unfolding events with a ΔLc value of 6.8 nm correspond to the rupture of the Fe−Cys41 bond and the subsequent extension of the inserted loop.).

(38) Eaton, W. A.; Lovenberg, W. *Iron-Sulfur Proteins*; Academic Press: New York, 1973.

(39) Notably, three new signals appeared only in the HSQC spectrum of the loop insertion variant. Consequently, we attribute these signals to the inserted loop. However, signals for most of the 19 residues of the inserted loop were not observed in our HSQC spectrum. Two factors are likely responsible for this observation: (1) the highly paramagnetic environment of Fe(III)−rubredoxin and (2) the flexible and largely disordered nature of the inserted loop. Fe(III)−rubredoxin is high spin and thus is highly paramagnetic. In such an environment, even a small fluctuation of amino acid residues can cause significant chemical shift variation, and together with the fast paramagnetic relaxation, signal broadening can be excessive. The inserted loop region is directly connected to the iron center at both ends, and the remaining residues are expected to be more flexible and largely disordered, so it is not surprising that most signals expected from this loop could not be observed.

(40) Carrion-Vazquez, M.; Oberhauser, A. F.; Fowler, S. B.; Marszalek, P. E.; Broedel, S. E.; Clarke, J.; Fernandez, J. M. *Proc. Natl. Acad. Sci. U.S.A.* **1999**, *96*, 3694.

(41) Marszalek, P. E.; Lu, H.; Li, H.; Carrion-Vazquez, M.; Oberhauser, A. F.; Schulten, K.; Fernandez, J. M. *Nature* **1999**, *402*, 100.

(42) Cavagnero, S.; Zhou, Z. H.; Adams, M. W.; Chan, S. I. *Biochemistry* **1998**, *37*, 3377.

(43) It is important to note that the observation of 12 nm extension followed by 7 nm extension does not necessarily correspond to the simultaneous rupture of 5 + 8 S ligands, because we cannot distinguish

sequential rupture from concurrent rupture of the native C5XXC8 loop (the rupture of Fe−C5 will only lead to an extension of 0.72 nm). Instead, the observation of unfolding events of ΔLc of 12 nm + 7nm only indicates that the rupture of the Fe−S center is initiated from the C5XXC8 side.

(44) Peng, Q.; Li, H. B. *J. Am. Chem. Soc.* **2009**, *131*, 14050.

(45) Stahl, S. W.; Puchner, E. M.; Alexandrovich, A.; Gaute, M.; Gaub, H. E. *Biophy. J.* **2011**, *101*, 1978.

(46) Arnesano, F.; Banci, L.; Piccioli, M. *Q. Rev. Biophys.* **2005**, *38*, 167.

(47) Bertini, I.; Cowan, J. A.; Luchinat, C.; Natarajan, K.; Piccioli, M. *Biochemistry* **1997**, *36*, 9332.

(48) Xiao, Z. G.; Lavery, M. J.; Ayhan, M.; Scrofani, S. D. B.; Wilce, M. C. J.; Guss, J. M.; Tregloan, P. A.; George, G. N.; Wedd, A. G. *J. Am. Chem. Soc.* **1998**, *120*, 4135.

(49) Dietz, H.; Rief, M. *Phys. Rev. Lett.* **2008**, *100*, 098101.

(50) Eyal, E.; Dutta, A.; Bahar, I. *Wiley Interdiscip. Rev.: Comput. Mol. Sci.* **2011**, *1*, 426.

(51) Stacklies, W.; Vega, M. C.; Wilmanns, M.; Grater, F. *PLoS Comput. Biol.* **2009**, *5*, e1000306.

(52) Edwards, S. A.; Wagner, J.; Grater, F. *PLoS Comput. Biol.* **2012**, *8*, e1002509.

(53) Ribas-Arino, J.; Marx, D. *Chem. Rev.* **2012**, *112*, 5412.